Cryogenics 50 (2010) 167–176

Contents lists available at ScienceDirect

Cryogenics

journal homepage: www.elsevier.com/locate/cryogenics

The 4C code for the cryogenic circuit conductor and coil modeling in ITER

L. Savoldi Richard [a], F. Casella [b], B. Fiori [a], R. Zanino [a,*]

[a] Dipartimento di Energetica, Politecnico di Torino, Torino, Italy
[b] Dipartimento di Elettronica e Informazione, Politecnico di Milano, Milano, Italy

ARTICLE INFO

Article history:
Received 16 January 2009
Received in revised form 22 June 2009
Accepted 22 July 2009

Keywords:
Nuclear fusion
ITER
Superconducting coils
System code
Thermal-hydraulic modeling

ABSTRACT

A new tool – the 4C code – has been developed, which allows the thermal-hydraulic simulation of the entire superconducting magnet system of the International Thermonuclear Experimental Reactor (ITER), with particular reference to: (1) the winding made of cable-in-conduit conductors (CICC), (2) the structures (the radial plates and the case of the toroidal field – TF – coils, for instance) and (3) the cooling circuits. In this paper the different components of the 4C code (1D 2-channel model of the CICC and of the structure cooling channels, 2D model of selected cross sections of the structures, 0D/1D model of the cryogenic circuit) are described in detail, together with the strategy adopted for the coupling between the different components and their integration in a single tool. The new tool is then applied to the modeling of two transients in an ITER TF coil: a simplified version of a cooldown of the coil and the response to a heat pulse applied in the winding.

1. Introduction

As we move toward the construction of the International Thermonuclear Experimental Reactor (ITER) [1], the availability of numerical simulation codes for the thermal-hydraulic (TH) assessment of the operating scenarios of the reactor is an item of growing importance. These codes are often labeled "system codes" as they must include an adequate integrated description of several different sub-systems in the reactor, e.g., in the case we are considering here, the cryogenic system and the superconducting coils.

So far, basically only one tool, the Vincenta code [2], was extensively applied to such simulations for ITER; however, the numerical accuracy of Vincenta in 'intermediate' speed simulations is a concern, as well as its user interface and support, so that there is significant interest in developing a more modern thermal-hydraulic code [3]. An action in that direction was recently launched in the EU, aimed at developing a new tool as "supplement and backup to Vincenta"; the 4C code presented here is the result of that action.

The 4C code allows the TH simulation of the entire ITER magnet system, with particular reference to the winding made of cable-in-conduit conductors (CICC), the structures (the radial plates and the case of the toroidal field – TF – coils, for instance) and the refrigeration circuit.

In perspective this tool is aimed at predicting the coil performance in terms of temperature margin and the overall heat loads to the cryoplant, as well as at simulating the control of the helium flows to, e.g., smooth the pulse load in the cryoplant.

In the paper, the different components of the code (1D multi-region model of the CICC and 1D model of the structure cooling channels[1], 2D model of selected cross sections of the structures, 0D/1D model of the cryogenic circuit) are described in detail together with the coupling between the different components and their integration in a single tool.

The 4C code is then applied to the modeling of two simple transients in an ITER TF coil, see Fig. 1a. The ITER cryogenic circuit design presently foresees, for the TF magnet system, two parallel cooling circuits, one for the winding and one for the case, see Fig. 1b (the model presented here extends that in [4] by including also the coil case and the respective cooling circuit). The two circuits are modeled simultaneously with the 4C code: the circuit for the cooling of the winding is coupled to the winding itself (14 CICC pancakes) and to the radial plates, while the case circuit is coupled to the case structures; the thermal coupling between winding pack and case is also accounted for.

2. The 4C model

The target of the simulations presented in this paper is an ITER TF coil and its cooling circuits as shown in Fig. 1.

* Corresponding author.
E-mail address: roberto.zanino@polito.it (R. Zanino).

[1] The CICC is divided in several macro-regions on the cross section (e.g., central channel, strands, annular channel, jacket) and for each of these, as well as for the case-cooling channels, only the longitudinal coordinate is discretized numerically.

0011-2275/$ - see front matter © 2009 Elsevier Ltd. All rights reserved.
doi:10.1016/j.cryogenics.2009.07.008

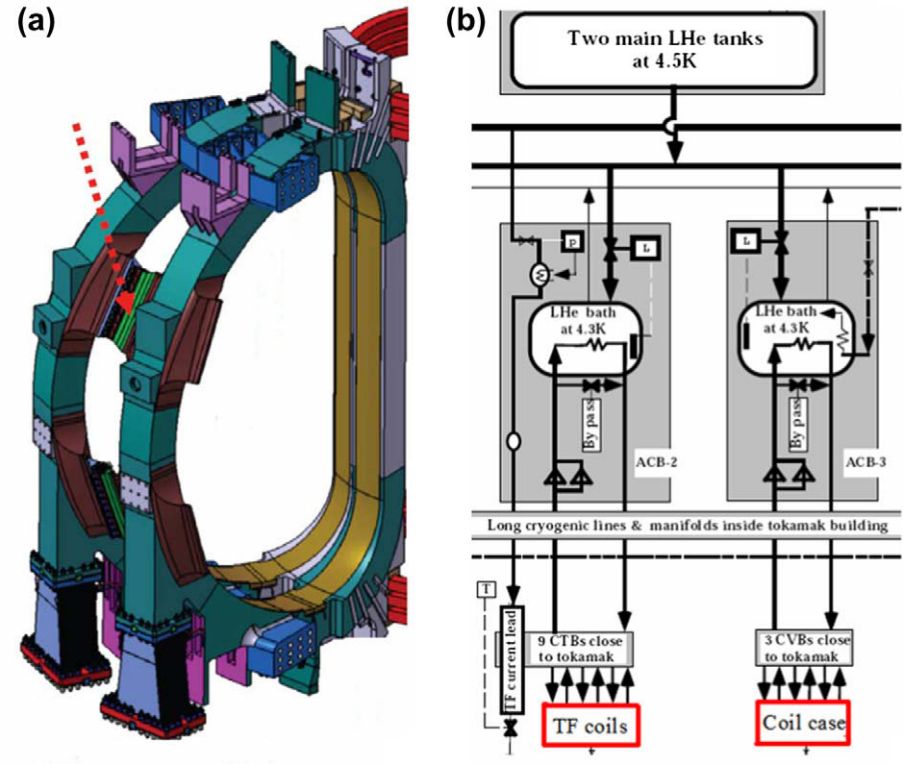

Fig. 1. (a) ITER TF coils (reproduced from [1]) and (b) respective part of the cooling circuit (reproduced from [5]).

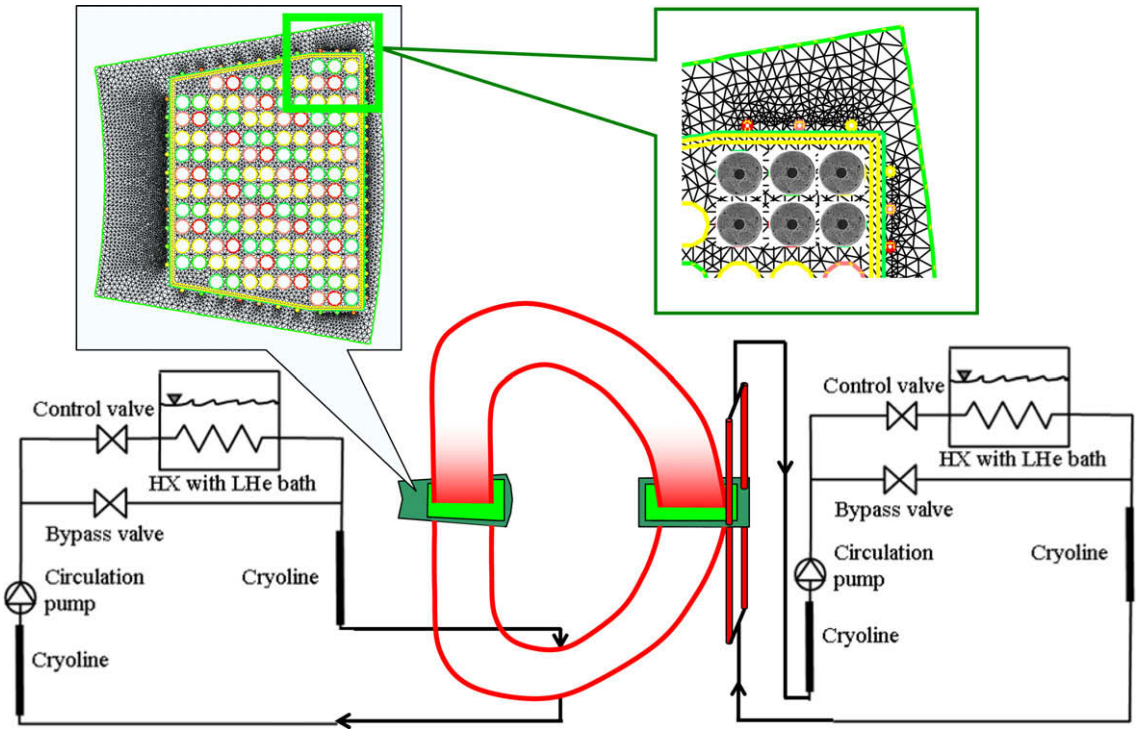

Fig. 2. Schematic representation of 4C code components: TF coil, structures and cooling circuits. Top left: inboard leg cross section; top right: zoom showing CICC, case cooling channels and 2D triangulation of the structures; bottom left and right: winding and case cooling circuits, respectively.

We see that two separate cooling circuits are devoted to the superconducting coils (i.e., the 18 winding packs each made of 14 CICC pancakes and radial plates) and to the coil case, respectively. The two circuits are similar in that both include a LHe bath at 4.3 K, a by-pass valve allowing its exclusion from the circuit, an auxiliary cold box (ACB), circulation pump(s) and long cryolines. The scope of our modeling as presented here does not include the whole cryoplant but stops at the heat exchanger with the LHe bath.

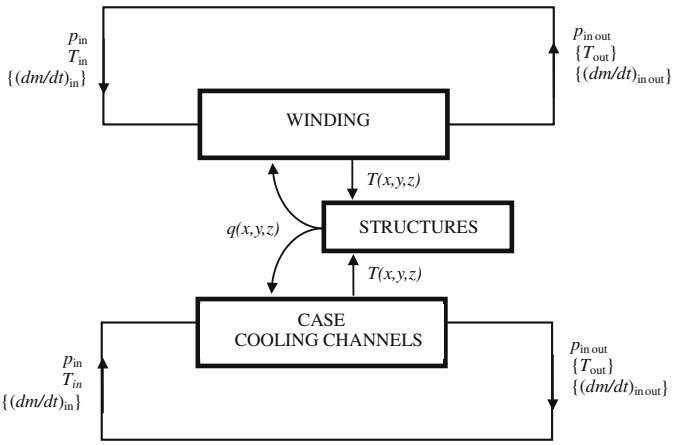

Fig. 3. Interfaces and boundary conditions in the 4C model. Quantities in braces are transferred from the winding and case-cooling channel models to the circuit models.

4C models the system as described in Fig. 2. While the details of the CTBs and CVBs have not been included so far, and the flow control is lumped in the "control valve", the main features of the circuit (pump, heat exchanger HX with the helium bath, cryolines) are simulated by the circuit model. The CICC constituting each pancake are included, as well as the cooling channels in the case. The "structures", i.e., coil case and radial plates, which are essential to properly describe thermal transients because of their large heat capacity, as well as being subject to the heat deposition by neutrons and eddy currents, are also accounted for. They are simplified in the model by down-scaling discretizing the corresponding 3D heat conduction problem in an adequate series number of 2D cuts (so-called 2½-D model).

The main model components included in 4C are:

- 1D transient thermal-hydraulic analysis, for the conductor winding [6] and the case-cooling channels;
- 2½-D heat conduction based on the public software Freefem++ [7], for the radial plates and coil case;
- 1D compressible flow model in cryolines/and HX + 0D (lumped-parameter) mass and energy balances in valves, and pumps, . . . , based on the Dymola commercial software [8], and on the ThermoPower library [9,10] for the cryogenic cooling circuits;

while the synchronization and coupling between (winding + case-cooling channels + radial plates + coil case) and cryogenic cooling circuits is performed via the commercial TISC software [11].

The different components are coupled through the definition of interfaces and boundary conditions as shown in Fig. 3.

The coupling between winding (CICCs) or case-cooling channels and the circuit is explicit in time, as explained below. The winding (CICCs) and case-cooling channel models require at each time step $t \rightarrow t + \Delta t$ the value of the inlet temperature T_{in} and pressure p_{in}, together with the outlet pressure p_{out}. This information is provided by the circuit model at fixed times $t_{exchange}$ (controlled by the TISC platform), and kept fixed between two subsequent exchange times (as their difference is always $\geqslant \Delta t$). At $t = t_{exchange}$ the winding (CICCs) and case-cooling channel models provide in turn the value of the inlet and outlet mass flow rates $(dm/dt)_{in}$, $(dm/dt)_{out}$, as well as the outlet temperatures T_{out} to the circuit models. The latter (averaged) value is computed from the values at the outlet of each channel, such as to reproduce the total enthalpy outflux, for the given p_{out}. The same applies in case of a backflow.

The coupling between the winding/case-cooling channels and the structures is performed at each time step according to the following strategy: the computation of the thermal-hydraulic transient in the winding/case-cooling channels is frozen at each time step t, while the heat conduction equation in the structures advances from t to $t + \Delta t$, using the jacket/pipe temperature $T(x, y, z, t)$[2] at the interface between winding and radial plates, for instance, in the evaluation of the boundary conditions, see below. Once the heat flux $q(x, y, z, t)$ from the structure has been computed, the execution of the winding/cooling channel model is restarted, using $q(x, y, z, t)$ as a heat source from t to $t + \Delta t$.

2.1. Model of the TF winding

A cross section of the TF winding is shown in cross section in Fig. 4a. There are 14 pancakes, the first and last made of three turns

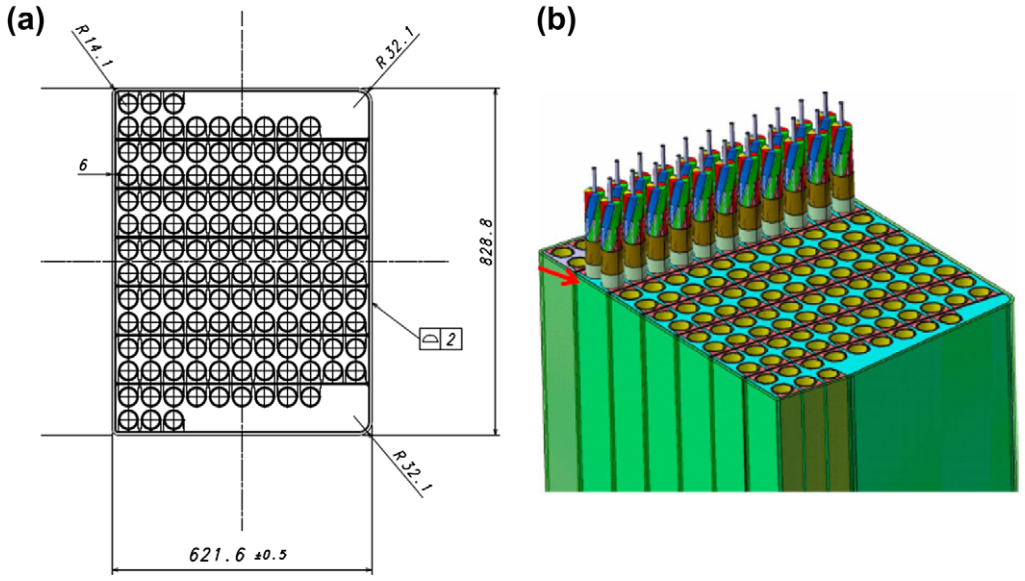

Fig. 4. (a) Outboard leg cross section of the ITER TF winding pack along on the equatorial plane of the machine (reproduced from ITER technical documentation). (b) Sketch of the inboard ITER TF winding pack (reproduced from [1]).

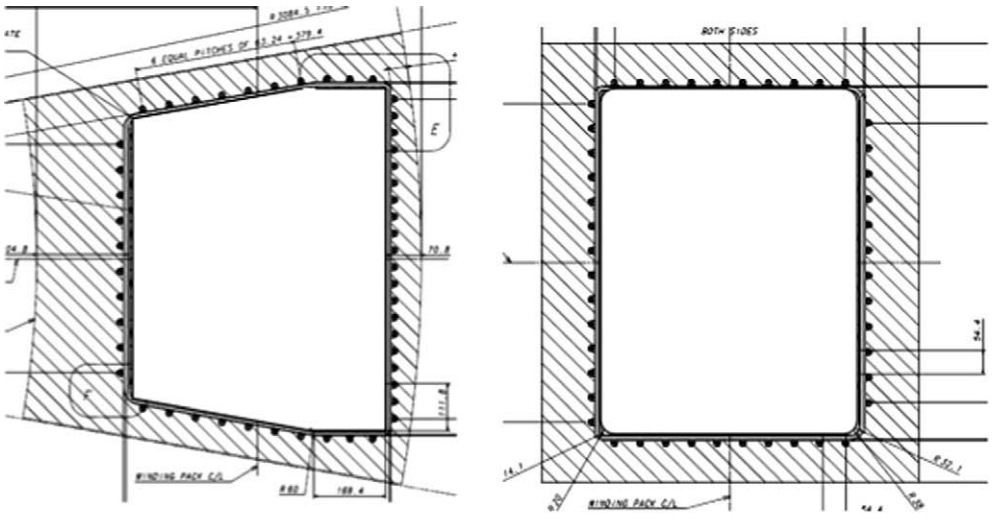

Fig. 5. TF coil case cross sections (inboard on the left, outboard on the right) on the equatorial plane of the tokamak. Reproduced from ITER technical documentation.

(hydraulic length ~99 m), the second and last but one made of nine turns (hydraulic length ~297 m), the rest made of 11 turns (hydraulic length ~363 m). Each pancake is modeled as in Mithrandir [6], a Fortran code including compressible (Euler-like) 1D He flow in central channel and annular region at different T and p, 1D heat conduction in the strands and in the jacket separately. The jacket is thermally coupled to the radial plates in a number of selected cuts: the jacket temperature is used to provide the convective heat flux q to the 2D heat conduction model in the radial plates, as a (Robin-type) boundary condition:

$$q = hP(\overline{T}_{JK}(t_n) - T_{i,j,s}(t_{n+1})) \quad (1)$$

where h is the heat transfer coefficient between winding/case-cooling channels and structures; h is computed from the thermal resistance due to the insulation layer wrapped around the jacket, which is not accounted for in our FE model (the heat capacity of the insulation layer is negligible anyway, in view of its very small volume); P is the wetted perimeter (i.e., the circumferential length of the interfaces between each conductor turn and the structures), $\overline{T}_{JK}(t_n)$ is the jacket temperature at the time t_n, averaged along each conductor turn and between the locations of the structure cuts, $T_{i,j,s}(t_{n+1})$ is the temperature of each boundary node of the sth structure on the jth turn of the ith conductor, at the time $t_{n+1} = t_n + \Delta t$. $T_{i,j,s}(t_{n+1})$ is then averaged for each turn of each conductor on each of the structure cuts, and used to compute an average heat flux $\bar{q}$, which is interpolated along each conductor and used to compute a volume heat source distributed in the jacket of the different pancakes when going from t_n to t_{n+1}.

The hydraulic inlet of the winding is located on the inner part of each section, where all 14 pancakes are present (left side of Fig. 4a, for instance), at the bottom of the coil (see Fig. 2).[3]

2.2. Model of the case-cooling channels

The case-cooling channels are shown in two equatorial cross sections in Fig. 5. There are 96 channels in total: 50 on the left (inboard) cross section, 46 on the right; the cooling of the case is done by separate parallel circuits for the inboard and outboard leg, from bottom to top.

[3] The clockwise/counterclockwise direction of the refrigeration along the adjacent pancakes has not been taken into account so far. Here we assume the flow to be counterclockwise in all pancakes.

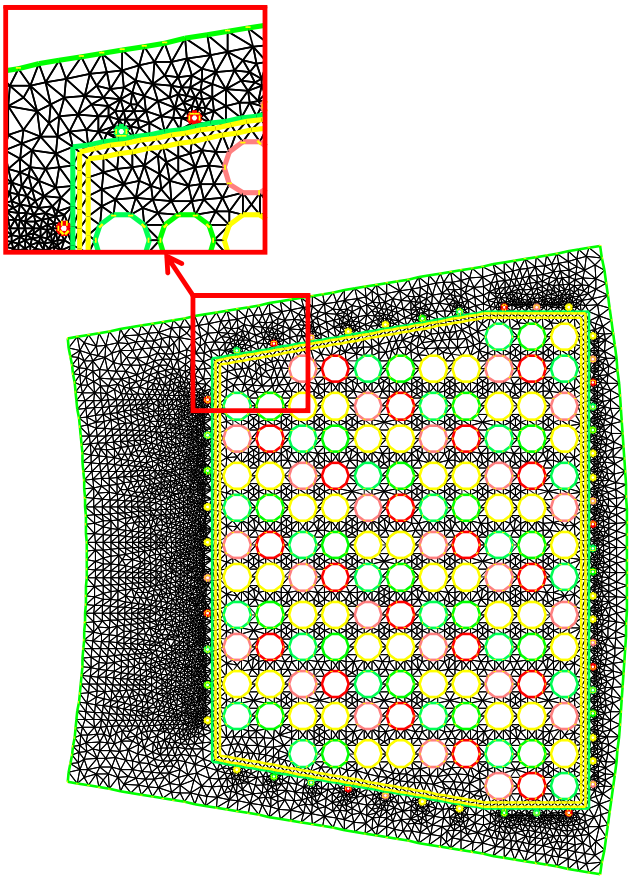

Fig. 6. Example of triangular mesh used for the solution of heat conduction problem in the structures (in this case the TF inboard leg). The colors are assigned by the software to distinguish different boundary tracts for computational purposes only.

The model describes the 1D compressible (Euler-like) flow in each channel, coupled to the 1D transient heat conduction along the cooling pipe through a Dittus–Boelter heat transfer coefficient. Each cooling pipe is then thermally coupled also to the case structure, in the same selected cuts used for the winding and following the same strategy described above.

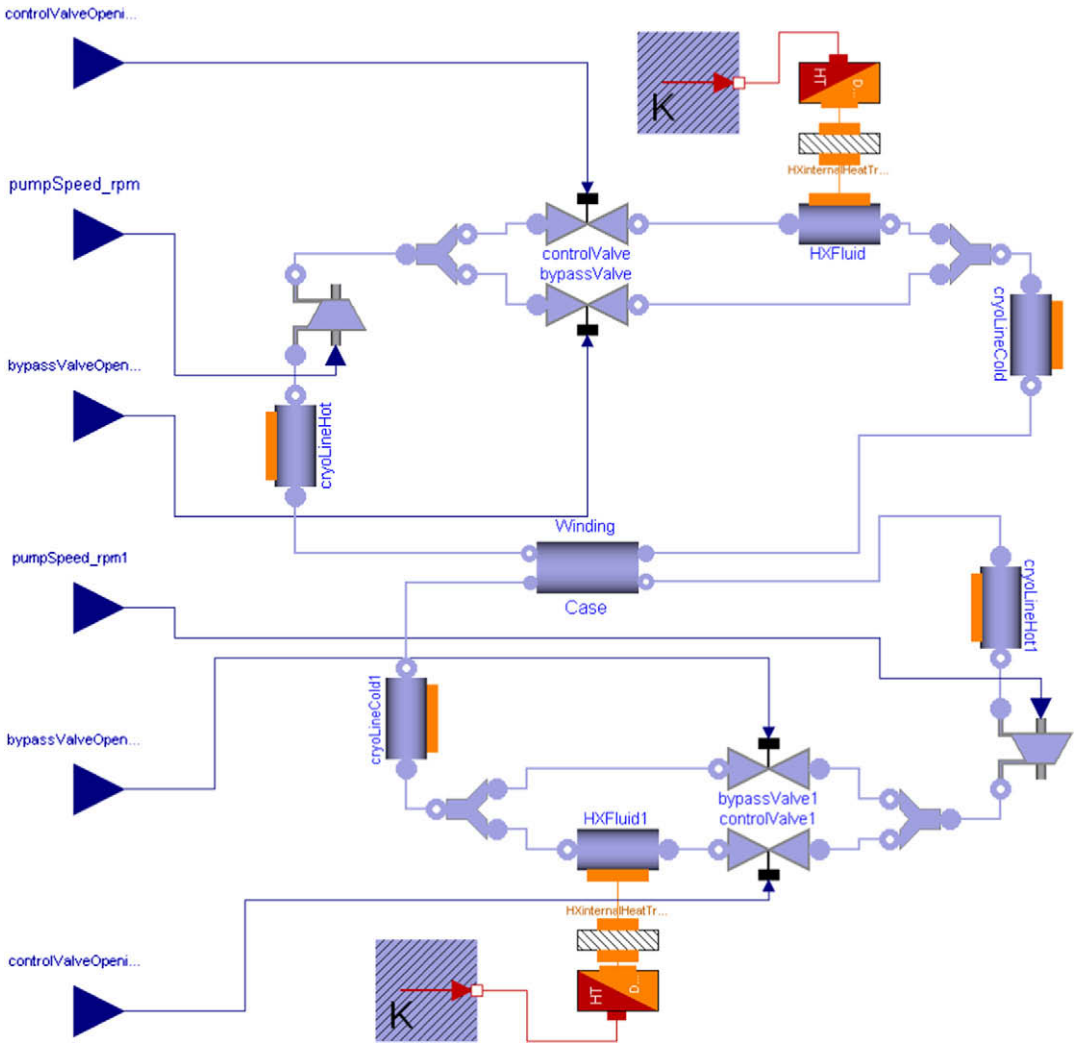

Fig. 7. Model of the cooling circuit built with ThermoPower components.

2.3. Model of the radial plates and case structures

The 3D problem of heat conduction in radial plates and case structures is modeled by approximating it with a series of 2D problems to be solved on a number of cuts at selected poloidal locations, coupled by heat advection in the third (poloidal) direction along winding and case-cooling channels (the heat conduction in radial plates and case structures in the poloidal direction can be shown to be negligible with respect to He advection). We call this approach a 2½-D model.

On each selected cut a triangular grid is generated, see Fig. 6, and the finite element method is used to solve the transient heat conduction problem. This gives us the maximum flexibility in describing the details of the structures (e.g., insulation layers, circular conductors, wedged shape, etc.), whenever needed. Furthermore, material properties are implemented as functions of the local temperature.

The problem is simultaneously solved in radial plates and case, i.e., a single mesh is used for both and no numerical interface is needed, see Fig. 6. For the sake of simplicity, internal details of the radial plate structure such as insulation layers were not considered here; their inclusion in the present model would be straightforward, at the only expense of increased CPU time due to the needed increase in resolution of the grid.

At the boundary with the pancakes and/or the case-cooling channels, the temperature computed by the model of those components is used as Robin boundary condition, see above. At the case outer boundary, adiabatic conditions are assumed.

2.4. Model of winding and coil case cooling circuits

The diagram of the simplified circuit used at present to model the winding cooling circuit and the case cooling circuit is shown in Fig. 7.

The circuit is modeled using the object-oriented, equation-based modeling language Modelica [12,13], by assembling components from the ThermoPower library [9,10], which have been adapted in order to use the same helium properties used for the rest of the model. The Modelica model is then compiled into simulation code by the commercial software Dymola.

A limited number of circuit components have been considered so far:

- Valve → assuming adiabatic, isenthalpic flow, with the standard flow equation for compressible fluid valves;
- Pump → assuming an ideal isentropic transformation, with given hydraulic characteristic, defined by the user (currently linear), and rotational speed depending on the input signal;
- Heat exchanger and cryoline → for these components one-dimensional mass, momentum and energy balance equations (in the p, T, v variables, where v is the flow speed), are solved with the finite volume method. The inertial term in the momen-

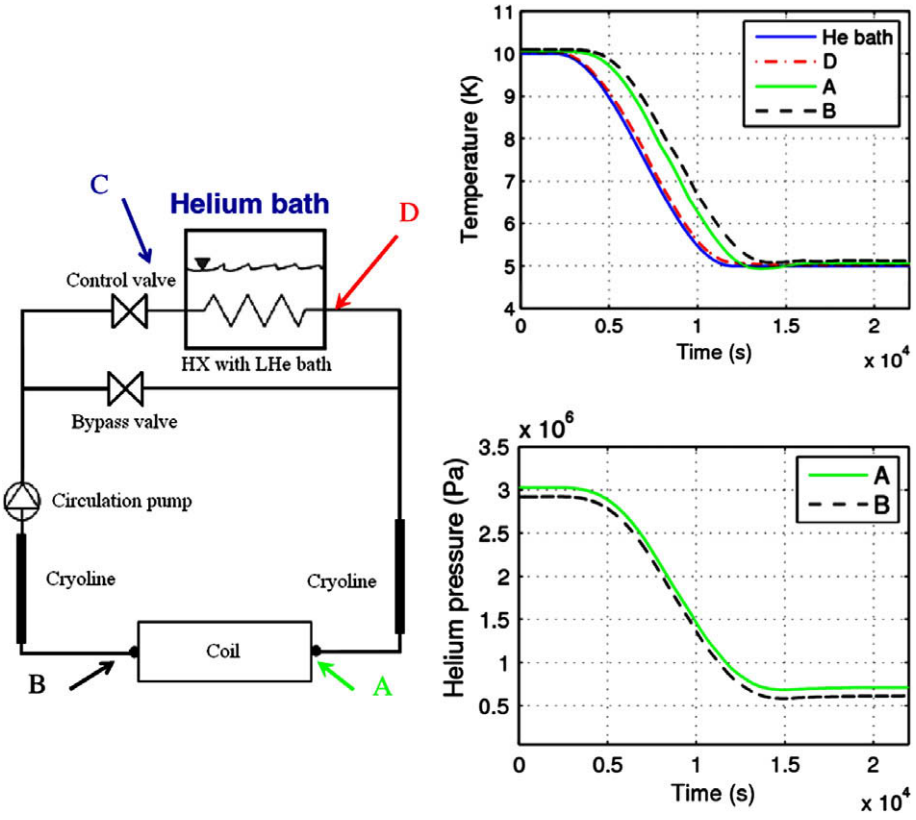

Fig. 8. Pseudo cooldown: Evolution of temperatures and pressures at the locations of the winding cooling circuit showed in the sketch on the left.

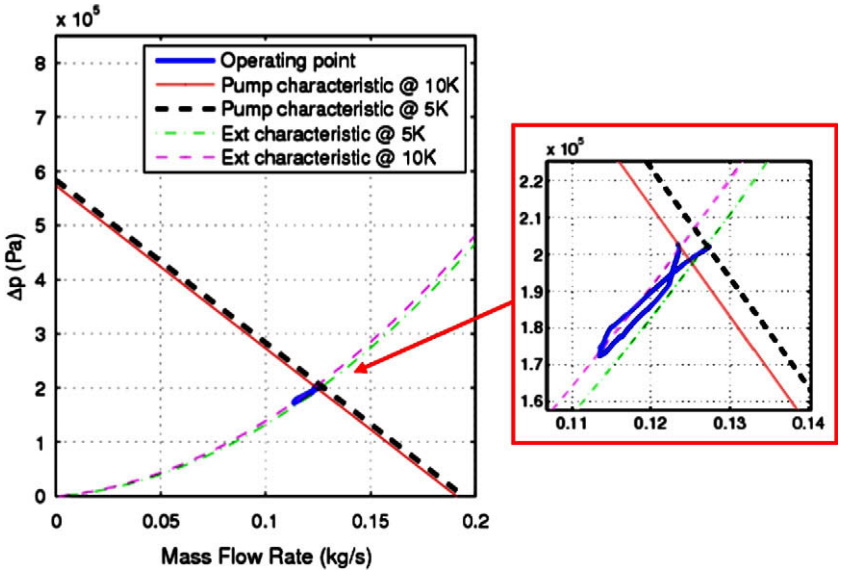

Fig. 9. Pseudo cooldown: Hydraulic characteristic of winding cooling circuit and pump. The inset shows a zoom near the operating point, in blue the trajectory of the system during the transient is shown.

tum balance is neglected, as the wave dynamics is not relevant in this context. The orange thermal connectors on the component side, which carry the vectors of nodal values of heat flux and fluid temperature, describe the heat transfer across the lateral tube boundaries. If there is no connection, zero heat flux is assumed, as it is the case of the insulated cryolines, and only fluid transport is modeled. In the case of the heat exchanger, the heat flux is computed by the connected convective heat transfer component, which has access to both the fluid temperatures inside the tubes, and to the fluid temperatures in the helium bath. The heat capacitance of the tube walls is currently neglected; it could be easily included at a later stage by connecting an extra component between the model of the fluid inside the pipe and the model of the helium bath;

- Helium bath → it is currently modeled as a fixed temperature source (icon with a K and arrow in Fig. 7). Since this standard component has a lumped-parameter thermal connector, carrying scalar temperature and heat power, a lumped/distributed adaptor (red/orange objects in Fig. 7) is used to connect it to the heat transfer model mentioned above, which has a distrib-

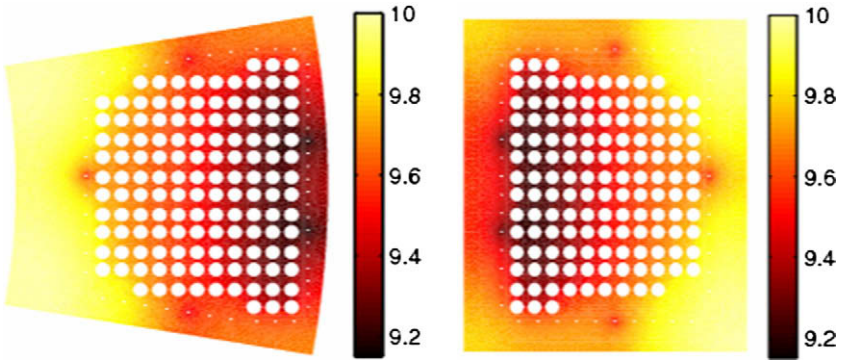

Fig. 10. Pseudo cooldown: Temperature distribution in the cross section of the coil radial plates and case at $t = 7000$ s.

Table 1
Pseudo cooldown: Results of conservation of mass and energy, interval, in the (2000 s, 32,000 s).

	Winding circuit	Case cooling circuit	Total
Mass (kg)			
Initial	660	409	1069
Final	679	420	1099
Energy (MJ)			
Q heat exchanger	−12.88	−9.758	−12.593
L pump	6.029	4.016	
ΔU structures	−5.738		−12.597
ΔU helium	−6.859		

uted-parameter connector; this model transfers the scalar temperature on one connector to the vector of temperatures on the other, and integrates the heat fluxes on the distributed connector into the lumped heat power on the lumped connector. A more detailed two-phase volume model is envisioned for the future, accounting for the changes in the helium temperature due to evaporation and condensation.

The coupling with the winding/cooling case model requires an additional component (shown at the center of the diagram in Fig. 7) that contains the interface with the commercial TISC software, allowing the needed exchange of variables. It acts as a boundary condition between the Modelica model of the cooling circuit, and the Fortran model of the windings, by sending and receiving values for helium pressure, temperature and mass flow rate at its ports whenever $t = t_{\text{exchange}}$.

Each component is described in terms of differential and algebraic equations (DAEs), written in the Modelica language, relating the internal variables and the connector (or port) variables which describe its boundary conditions: pressure, mass flow rate and specific enthalpy for fluid ports (full and hollow round connectors in Fig. 7), temperatures and heat flows for thermal ports (rectangular connectors in Fig. 7). The connection between two ports corresponds to additional equations added to the system, stating that "flow" variables (mass flow rate, heat flow) sum to zero, and "effort" (i.e., not-flow) variables (pressure, temperature) are equal on the two connectors. Specific enthalpy requires a special treatment described in detail in [9], to describe reversing flow situations.

The system model thus corresponds to a set of DAEs, containing both the component equations and the connection equations

$$F(\lambda,\ d\lambda/dt, \mu, \omega) = 0 \tag{2}$$

where λ is the vector of state variables, i.e., those which are differentiated in the model, μ is the vector of algebraic variables, i.e., those which are not differentiated in the model, and ω is the vector

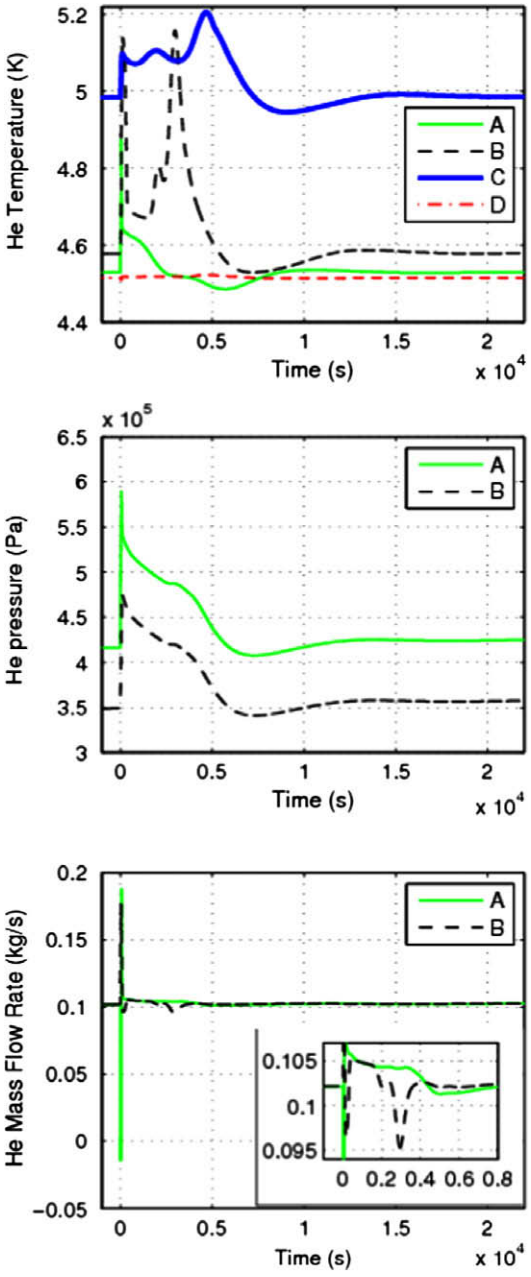

Fig. 11. Heat pulse in the winding: Evolution of pressures, temperatures and helium mass flow rates at different winding cooling circuit location.

of exogenous inputs, i.e., the variables coming from the coupled winding/cooling case model, and the control variables (valve openings, pump speed).

This set is then processed by Dymola in order to transform it into state-space form

$$\begin{aligned} d\lambda/dt &= f(\lambda,\omega) \\ \mu &= g(\lambda,\omega) \end{aligned} \tag{3}$$

In order to do this efficiently, symbolic and numeric algorithms are used. More details on this process can be found in [13].

The outcome of this process is a C source code, which is then linked to the DASSL-RT solver [14] integrating the differential equations over the time intervals required by the TISC interface.

The modularity of the object-oriented modeling approach makes this model very flexible, enabling the user to later change some of the components by substituting them with more detailed counterparts. Furthermore, adding customized models is made easy by the equation-based approach, which allows one to write any kind of describing differential-algebraic equations without bothering about how to solve them.

3. Results and discussion

Two simple applications of the code are considered here in some detail, in order to give a first demonstration of the capabilities and accuracy of 4C:

- A (drastically) simplified version of the cooldown of the coil, defined below as pseudo cooldown, in which the temperature of the LHe bath is slowly decreased from 10 K to 5 K in a closed thermodynamic cycle.
- The response of the system to a heat pulse applied to a portion of the winding.

In both cases the by-pass valve is closed.

3.1. Application 1: pseudo cooldown

The driver for this transient is the simultaneous reduction of the temperature of the LHe bath from 10 K to 5 K in ~10,000 s (i.e. at a rate of ~2 K/h) in both cooling circuits. Two poloidal cross sections (cuts) for heat conduction in the radial plates are considered, on the equatorial plane of the coil. A first set of results for this simulation is shown in Fig. 8.

As expected, the temperatures follow the driver until a new steady state is reached (note that the outlet temperature is higher than the inlet because of the Joule–Thompson effect). The delay with which the cryoline temperature decreases is much longer than that of the winding pack + coil case. Considering the difference of masses and hydraulic lengths involved, such behavior is at first sight quite surprising, but it can be easily explained by referring to the similar case study which was presented in [4], where however the coil case was not included. In that case [4] the delay in the decrease of the temperature at the winding outlet was indeed somewhat longer, because of the longer transit time, than the delay at the cryoline outlet. This suggests that the behavior shown in Fig. 8 is actually due to the presence of the coil case in this simulation: the transit time in the case-cooling channels is much shorter than the transit time in the winding, and the two components are well thermally coupled in the present model, such that the fast decrease of the case temperature (not shown here) pulls down also the winding temperature.

The pressure in the circuit decreases from 3 MPa to well below 1 MPa, as a consequence of the need to conserve the total He mass and volume, since the loop is closed: then a pressure reduction, concomitant with the temperature reduction, is needed to maintain the average density constant.

In both the initial and the final steady state, the operating condition (in terms of mass flow rate dm/dt, and pressure drop Δp) for the pump/circuit is obtained by the intersection of the pump forcing characteristic with the resistive characteristic of the circuit component, due to the finite friction in cryolines and winding, as shown in Fig. 9. In view of the small change of both forcing and resistive characteristics between the initial and the final condition, basically due to the conservation of the average density during the transient, the mass flow rate dm/dt is almost constant during the transient.

The computed temperature distribution in radial plates and case near the middle of the transient ($t \sim 7000$ s) is shown in Fig. 10. The effect of colder turns close to the He inlet on the inner

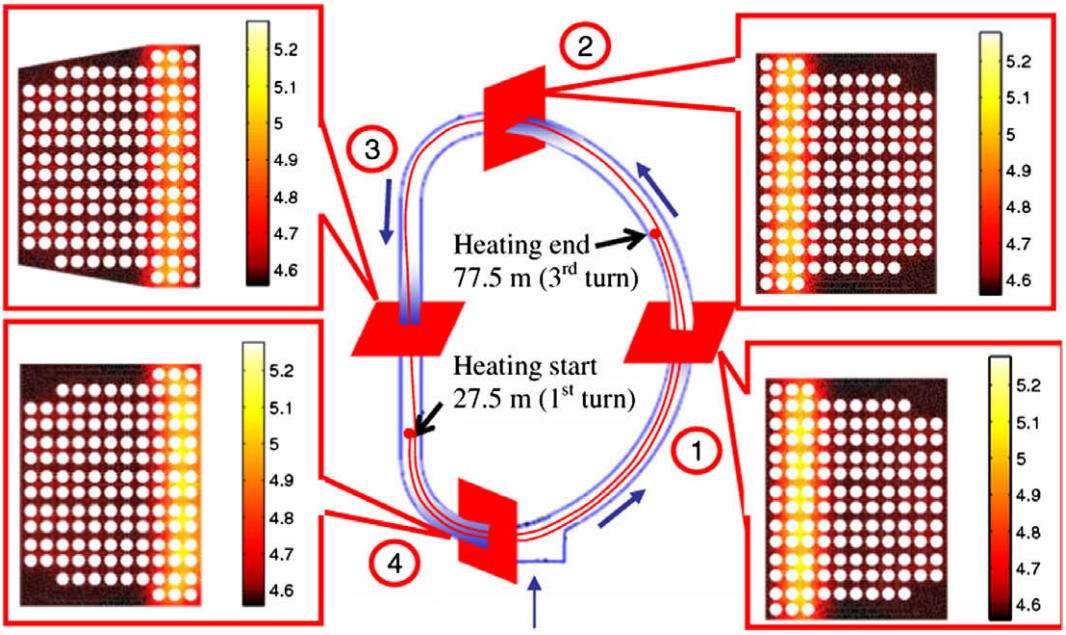

Fig. 12. Heat pulse in the winding: Temperature distribution in the cross section of the coil radial plates at $t = 100$ s.

side of the coil is clear, as well as the sink effect of the case-cooling channels (note that in this example, for the sake of shortening the CPU time, only five case-cooling channels are "active", which are clearly noticeable in the figure, whereas the rest of the cooling channels is assumed adiabatic).

In the transient under consideration the total mass in both the winding and the case cooling circuits must be conserved at any time, as they are closed in the present model. We see in Table 1 that this conservation is verified by the code to good (~3%) accuracy, between the initial and final time of the transient. This small residual error is a consequence of the use of different grids for the linear interpolation of different helium thermo-physical properties in the (p, T) plane [15]. This grid mismatch introduces a little inconsistency in the evaluation of those properties which are not independent of each other (for instance, the density ρ and its derivatives, contained in the Gruneisen parameter φ [16]). This affects both the mass conservation in the cryolines, which is solved directly in the form: $dM/dt = \int \left[(\partial\rho/\partial p)_T \times dp/dt + (\partial\rho/\partial T)_p \times dT/dt\right] dV$, where M is the mass and V the volume, and the solution of the helium flow model in the winding and in the case-cooling channels, where the conservation equations are written in the non-conservatives variables v, p and T, with ρ and φ appearing as coefficients. Also the first principle of thermodynamics (conservation of energy) must obviously be satisfied by our solution, i.e., $L + Q = \Delta U$, where L is the work done on the coolant by the pumps, Q the heat received by the coolant at the heat exchanger and ΔU the variation of internal energy of structures and coolant. Indeed, we see in Table 1 that

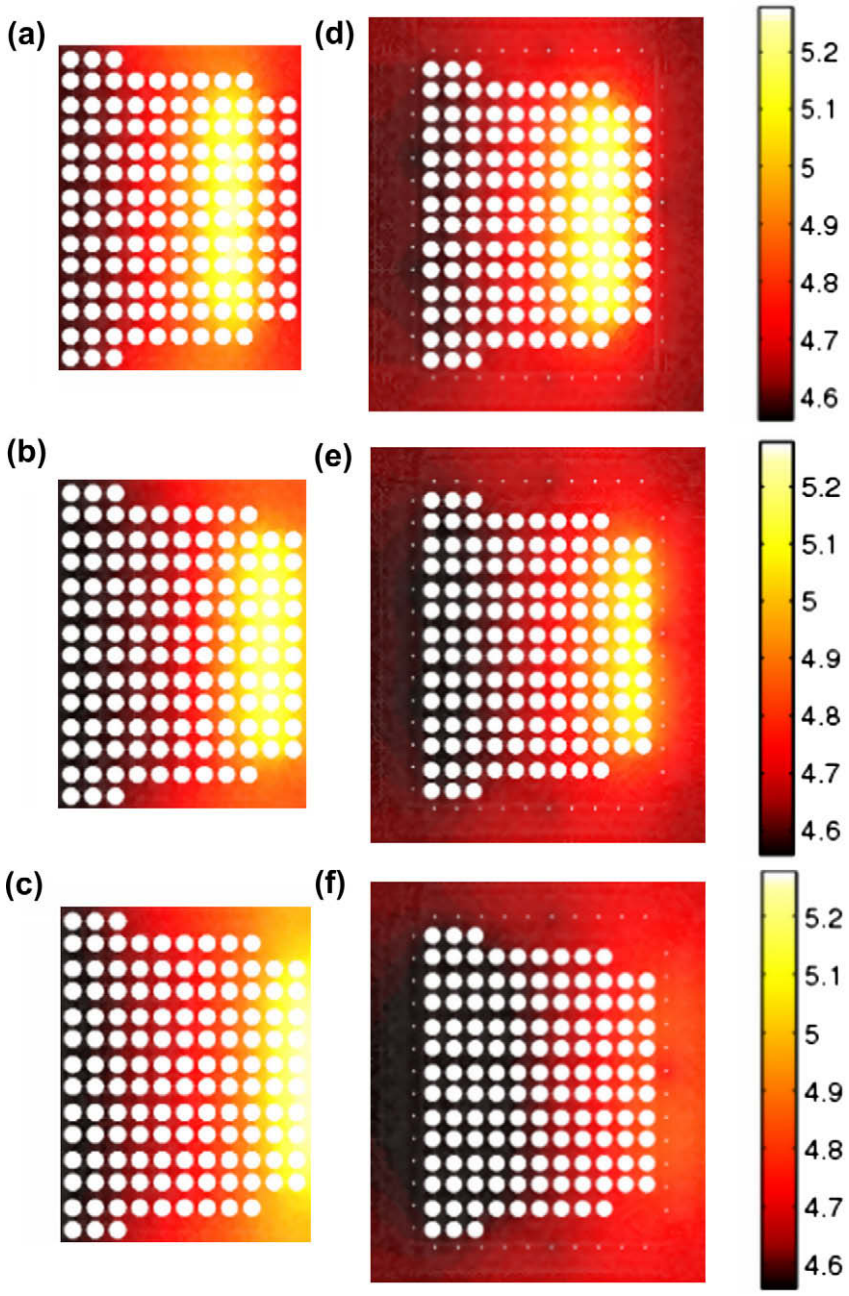

Fig. 13. Heat pulse simulation in the winding: Temperature distribution computed in the outboard section without the case (a, b, c) and with the case (d, e, f), at t = 2000 s, 2500 s, 3000 s, respectively.

Table 2
Results of conservation of mass and energy, interval (0 s, 22,000 s).

Mass (kg)		
Initial	670.2	
Final	671.7	
		Total
Energy (kJ)		
Q driver	350.0	
Q heat exchanger	−5065	14.16
L pump	4729	
ΔU structures	0.3102	14.06
ΔU helium	13.75	

the total energy in the system is conserved by the code to good accuracy.

3.2. Application 2: heat pulse in the winding

The driver for this transient is a square wave heat pulse in the winding (10 w/m for 50 s, along 50 m centered around on the 2nd turn). The coil case is initially not included in the simulation of this application, whereas four poloidal cross sections (cuts) in the radial plates are considered, as opposed to the two of the previous example, at 90° from each other (the winding cross sections at the two new cuts have been considered for the sake of simplicity as identical to the outboard cross section on the equatorial plane).

The evolution of pressures, mass flow rates and temperatures for this case is shown in Fig. 11, with the same circuit reference points as in Fig. 8. As a result of the heat pulse, the system pressurizes and backflow of hot He at the inlet of the coil occurs. At the outlet of the coil, three peaks appear in the temperature during the transient, as a consequence of the three different hydraulic lengths in the winding, see Fig. 4a (a similar effect is seen in the three peaks appearing in the outlet mass flow rate, as the temperature increase, combined with a pressure decrease, directly reflects into a density reduction).

In Fig. 12 the temperature distribution at $t = 100$ s in the four cuts of the radial plates are reported. The distribution directly reflects the poloidal location of the source, which affects cut "1" in the 2nd and 3rd turns, cuts "2" and "3" only in the 2nd turn and finally cut "4" in the 1st and 2nd turn.

The temperature distribution at the times at which the heat pulse exits the conductors with different lengths for the outboard cut on the equatorial plane is reported in Fig. 13, for the computation performed with two radial plate cuts and with/without the coil case. When the coil case is included in the simulation, a much higher diffusion in the solids is present, and the temperature peaks at the winding outlets are less visible than in the simulation without the case.

The relative difference between the maximum temperature computed on the radial plates with four cuts vs. two cuts stays below 2% in this case, where the maximum temperature increases by about 1 K, starting from about 4.5 K.

Also for this case, both mass and energy conservation are verified to good accuracy by the code, see Table 2.

4. Conclusions and perspective

The 4C code has been developed to model thermal–hydraulic transients in the ITER superconducting coils, including winding, structures and cooling circuit.

4C has been applied to two model problems in the case of an ITER TF coil (a simplified version of the cooldown of the coil and the response to a heat pulse in the winding), showing the capability to accurately simulate the thermal-hydraulic system evolution.

In perspective, we plan to:

- Benchmark 4C against the Vincenta code.
- Validate 4C against experimental data from, e.g., the ITER Model Coils, or other available data from superconducting tokamak operation.
- Apply 4C to ITER-relevant predictions.

Acknowledgments

The European Fusion Development Agreement (EFDA) partially financially supported this work, together with the Italian Ministry for University and Research (MUR). LSR acknowledges support from a "Giovani ricercatori" fellowship, while the Associazione per lo Sviluppo scientifico e tecnologico del Piemonte (ASP) partially financially supported the MSc thesis work of BF.

References

[1] Mitchell N, Bessette D, Gallix R, Jong C, Knaster J, Libeyre P, et al. The ITER magnet system. IEEE Trans Appl Supercond 2008;18:435–40.
[2] Bessette D, Shatil N, Zapretilina E. Simulations of the ITER toroidal field coil operation with the VINCENTA code. IEEE Trans Appl Supercond 2006;16:795–8.
[3] Mitchell N. The role of superconductor modeling in ITER, presented at the CHATS Workshop, October 30–November 1, 2008, Tsukuba, Japan.
[4] Savoldi Richard L, Casella F, Fiori B, Zanino R. Development of the cryogenic circuit conductor and coil (4C) code for thermal-hydraulic modeling of ITER superconducting coils. In: Chang Ho-Myung, et al., editor. Proceedings of the 22nd international cryogenic conference (ICEC22); 2009. p. 619–24.
[5] ITER Technical Basis, Cap. 3.2. Cryoplant and cryodistribution; 2001.
[6] Savoldi L, Zanino R. M&M: multi-conductor mithrandir code for the simulation of thermal-hydraulic transients in super-conducting magnets. Cryogenics 2000;40:179–89.
[7] Hecht F. FreeFem++ Manual, 3rd ed. Version 3.4-2. Laboratoire Jacques-Louis Lions, Universite' Pierre et Marie Curie, Paris, France ; 2009. Available from: http://www.freefem.org/ff++/ftp/freefem++doc.pdf.
[8] Dymola (Dynamic Modeling Laboratory) User's Manual, Version 5.3, DYNASIM AB, Lund, Sweden;2004.
[9] Casella F, Leva A. Modelling of thermo-hydraulic power generation processes using Modelica. Math Comput Model Dyn 2006;12:19–33.
[10] Casella F, Leva A. Modelica open library for power plant simulation: design and experimental validation. In: Proceedings 3rd international Modelica conference, Linköping, Sweden, November 3–4, 2003. p. 41–50.
[11] TLK – Thermo GmbH Braunschweig, Dymola interface for TISC-documentation; 2006.
[12] Mattson SE, Elmqvist H, Otter M. Physical system modeling with Modelica. Control Eng Pract 1998;6:501–10.
[13] Fritzson P. Principles of object-oriented modeling and simulation with Modelica 2.1. Wiley; 2003.
[14] Brenan KE, Campbell SL, Petzold LR. Numerical solution of initial-value problems in differential algebraic equations, North-Holland; 1989.
[15] Zanino R, Bottura L, Savoldi L, Rosso C. Mithrandir+: a two-channel model for thermal-hydraulic analysis of cable-in-conduit super-conductors cooled with helium I or II. Cryogenics 1998;38:525–31.
[16] Zanino R, DePalo S, Bottura L. A two-fluid code for the thermohydraulic transient analysis of CICC superconducting magnets. J Fus Energy 1995;14:25–40.